Cell

Paradoxical Signaling by a Secreted Molecule Leads to Homeostasis of Cell Levels

Yuval Hart,[1,3] Shlomit Reich-Zeliger,[2,3] Yaron E. Antebi,[2,3] Irina Zaretsky,[2] Avraham E. Mayo,[1] Uri Alon,[1] and Nir Friedman[2,*]
[1]Department of Molecular Cell Biology, Weizmann Institute of Science, Rehovot 76100, Israel
[2]Department of Immunology, Weizmann Institute of Science, Rehovot 76100, Israel
[3]Co-first author
*Correspondence: nir.friedman@weizmann.ac.il
http://dx.doi.org/10.1016/j.cell.2014.07.033

SUMMARY

A widespread feature of extracellular signaling in cell circuits is paradoxical pleiotropy: the same secreted signaling molecule can induce opposite effects in the responding cells. For example, the cytokine IL-2 can promote proliferation and death of T cells. The role of such paradoxical signaling remains unclear. To address this, we studied $CD4^+$ T cell expansion in culture. We found that cells with a 30-fold difference in initial concentrations reached a homeostatic concentration nearly independent of initial cell levels. Below an initial threshold, cell density decayed to extinction (OFF-state). We show that these dynamics relate to the paradoxical effect of IL-2, which increases the proliferation rate cooperatively and the death rate linearly. Mathematical modeling explained the observed cell and cytokine dynamics and predicted conditions that shifted cell fate from homeostasis to the OFF-state. We suggest that paradoxical signaling provides cell circuits with specific dynamical features that are robust to environmental perturbations.

INTRODUCTION

Cells can interact with each other by secreted or cell surface signaling molecules forming functional cell circuits. In many cases, the signaling molecule has pleiotropic or even paradoxical antagonistic effects on the responding cells (Hart and Alon, 2013). For example, glucose has both mitogenic and toxic effects on pancreatic β cells (Dadon et al., 2012). In developing fly embryos, an inhibitor of the BMP morphogen also functions as a carrier, therefore increasing the morphogen range of activity (Eldar et al., 2002; Haskel-Ittah et al., 2012) and in the delta-notch signaling system, delta has opposite effects on its target notch, depending on whether notch is located on a neighboring cell or the same cell, allowing for sharp, short-range patterning (Sprinzak et al., 2010, 2011). In the immune system, many cytokines have paradoxical effects. The cytokine IL-27 promotes differentiation and also inhibits proliferation of T helper 1 (Th1) cells (Villarino et al., 2006). IL-2, a cytokine secreted by T cells upon antigen recognition, promotes T cell proliferation (Cantrell and Smith, 1984; Malek, 2008; Zhu and Paul, 2008) and also affects cell death (Deenick et al., 2003; Lenardo, 1991; Li et al., 2001; Refaeli et al., 1998). The existence of paradoxical extracellular signaling raises an important question: why do cells secrete a signaling molecule that has antagonistic effects? In other words, which cell circuit functions can be facilitated by paradoxical signaling?

An important function of cell circuits is maintaining homeostasis of cell concentration. Homeostasis requires a balance between proliferation and death rates. However, cell expansion processes are intrinsically sensitive to parameters that affect these rates (Hart et al., 2012). If the proliferation rate exceeds the death rate, cell numbers grow exponentially and only stop at the maximal carrying capacity; that is, the largest possible cell concentration under space limitations, confluence restriction, or the consumption of available growth resources. If the death rate exceeds the proliferation rate, the opposite occurs; cell counts drop to zero (Figure 1A). The intrinsic sensitivity of this simple expansion process raises the need for regulation of cell division and death rates. Specifically, regulation is needed to set the homeostatic cell density to be between the extinction level and the carrying capacity. Such regulation often involves the response of cells to paracrine and autocrine signaling that can be provided by neighboring cells or by the proliferating cells themselves (Youk and Lim, 2014). In the latter case, cells can respond to changes in their own levels. When a signaling molecule that is secreted and consumed by the same cells that it regulates has an antagonistic effect, changing both their proliferation and death rates, feedback mechanisms can arise (Figure 1B). Here we study the ability of such autocrine and paracrine feedback to keep the instability in check and lead to a stable level of cells.

Recently, the question of paradoxical pleiotropy (the ability of a cytokine to affect cells in opposite ways at the same time) was addressed using mathematical modeling of cell circuits (Hart et al., 2012). All possible patterns of connection between one cell type and a cytokine that affects cells' growth and/or death rate were analyzed. Paradoxical signaling, in which the cytokine increases

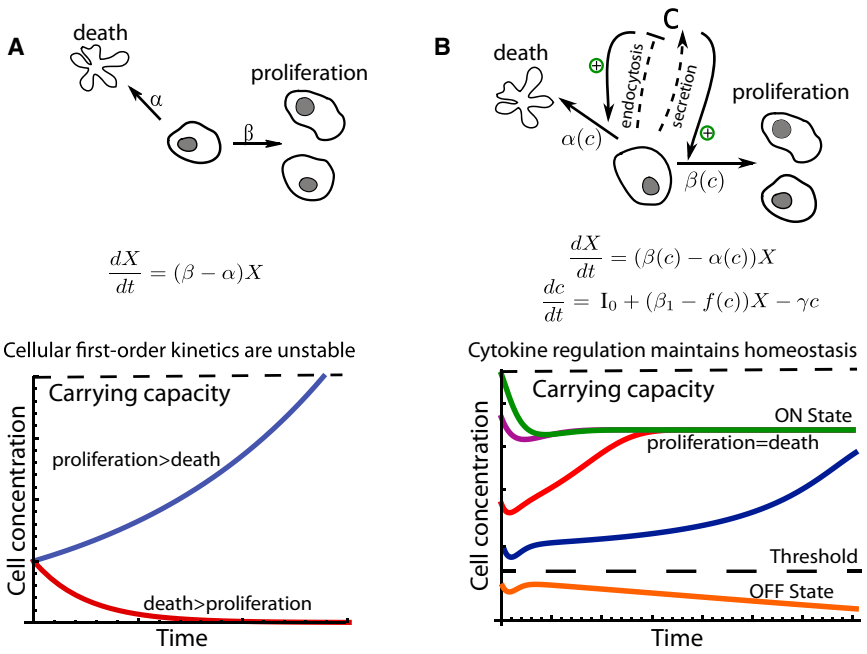

Figure 1. Schematic Models of Cell Proliferation and Death Are Fundamentally Unstable and Do Not Lead to Cell Number Homeostasis Unless Special Regulation Is in Place

(A) A simple, uncontrolled proliferation and death scheme leads to instability. If the proliferation rate (β) exceeds the death rate (α), the cell number (*X*) grows to high levels (up to the carrying capacity). If the opposite occurs, the cell number declines to zero. Homeostasis of cell number at intermediate levels lower than the carrying capacity is not possible.

(B) Homeostasis can be achieved when cell proliferation and death are regulated by a secreted molecule (denoted *c*) secreted by the cells (denoted *X*). For a wide range of initial cell levels, a final cell concentration is reached that does not depend on initial conditions. For very low initial concentrations, the cell number declines to zero (an OFF-state). β_1 is the rate of production of the molecule *c* by the cells, *f(c)* is its consumption rate, γ is its degradation rate, and I_0 is its external supply.

both proliferation and death rates, has been suggested to provide a specific dynamical feature to the circuit. Cells reach a homeostatic concentration, lower than the carrying capacity, that is robust to variations in initial cell numbers. In addition, if the initial population of cells is very low, the cell concentration declines to zero, which we call an OFF-state. In the specific case in which the cytokine is produced and consumed by the cells, homeostasis is accompanied by a temporal pulse of cytokine. Its level first increases and then decreases to a lower level when cell homeostasis is reached. Another prediction of the model is that, for homeostasis and an OFF-state to exist, the cytokine needs to affect either growth or death rates cooperatively (that is, in a sigmoidal manner) to create the potential for bistable dynamics.

Experimental studies of paradoxical extracellular signaling are generally challenging. A main difficulty is disentangling the conflated effects of the pleiotropic molecule because of the extracellular nature of the positive feedback and the interactions between the cells. Here, we use IL-2 signaling in $CD4^+$ T cells under persistent stimulation to investigate the design principles of paradoxical signaling and cell homeostasis. IL-2 affects T cell proliferation and death. It is secreted by T cells upon T cell receptor (TCR) stimulation and is consumed by activated T cells through binding to the IL-2 receptor, followed by internalization and degradation (Lamaze et al., 2001; Lan et al., 2008) (Figure 1B). Using this tractable in vitro model provides a simplified test bed to investigate this important natural signaling system without the full complexities of in vivo T cell signaling.

Here we show that mouse $CD4^+$ T cells cultured under persistent stimulation for 8 days with more than a 30-fold difference in initial cell levels reach a balanced homeostatic cell concentration that is nearly independent of initial levels. Homeostasis occurs only when the initial concentration is above a threshold concentration. When the concentration is below this threshold, the cell density decays, and the population becomes extinct (OFF-state). We further address the mechanism of homeostasis and find that it relates to the paradoxical effect of IL-2. IL-2 increases both proliferation and death rates; the latter by downregulating Bcl2. Specifically, we find that IL-2 increases the proliferation rate cooperatively and the death rate linearly; a relationship that, in the model, creates the bistable dynamics needed to provide both homeostasis and an OFF-state. We demonstrate how cell fate can change from the ON-state to the OFF-state by cell dilution, keeping IL-2 levels fixed as predicted by the model. Finally, we theoretically analyze an alternative case in which the dual effect of the paradoxical molecule is split into two distinct monofunctional molecules, one affecting cell proliferation and the other cell death. We find that, in this case, the full functionality of the circuit is achieved only in a narrow range of parameters and can be ruined by external supply or removal of the signal molecules. Therefore, the paradoxical design is important to insulate the circuit function from environmental perturbations.

RESULTS

$CD4^+$ T Cells Reach a Homeostatic Cell Concentration that Is Independent of Initial Cell Levels

We studied the dynamics of T cells in culture starting from different initial concentrations. Naïve mouse $CD4^+$ T cells were cultured in anti-CD3/anti-CD28-coated plates for 8 days. During the expansion process, we measured cell numbers (by flow cytometry), cell proliferation dynamics (by carboxyfluorescein succinimidyl ester [CFSE]), and IL-2 levels in the medium (by ELISA). Cultures showed three main subpopulations in flow cytometry analysis based on their forward and side scatter: naive, activated, and apoptotic cells (Figure S1A available online). Because the activated subpopulation was the predominant proliferative

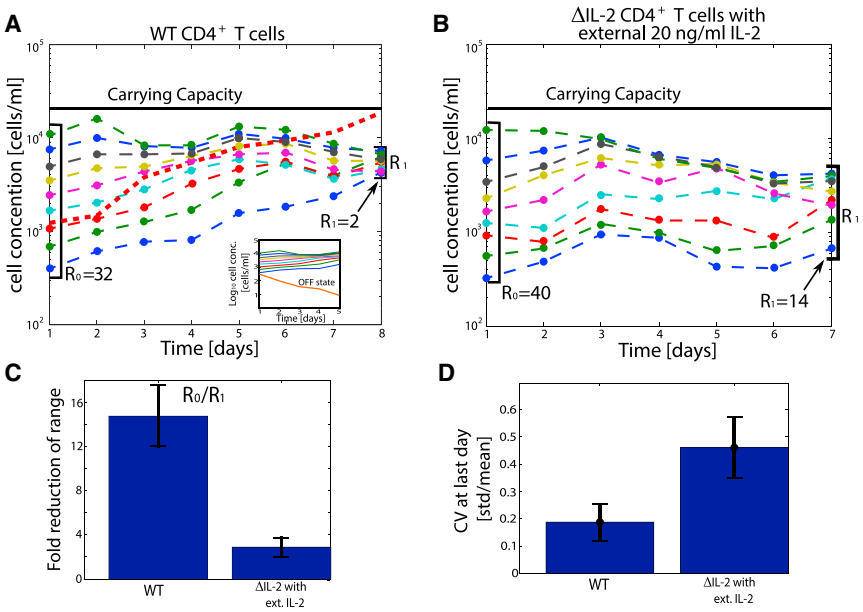

Figure 2. CD4⁺ T Cells Reach a Homeostatic Level Much Lower Than the Carrying Capacity in an IL-2-Dependent Manner

(A) Mouse naïve CD4⁺ T cells were stimulated by anti-CD3 + anti-CD28 for 8 days. The cell number was measured every 24 hr. Cells that were inoculated across a 32-fold range of initial concentrations reached a concentration after 8 days that spanned only 2-fold. This concentration was ~3-fold lower than the carrying capacity (lower bound), which was measured by CD4⁺ T cells grown under the same conditions but removed from stimulation at day 4 (dashed red line). Data are average over four repeated experiments (Figure S1C). In the inset, cells inoculated at low cell concentrations (below 320 cells/ml activated cells at day 1) declined to very low cell numbers (orange line).

(B) Mouse CD4⁺ T cells deleted for the IL-2 gene, were cultured in the same conditions as in (A) and were supplemented with 20 ng/ml external IL-2 added to the medium. Cells that were inoculated across a 40-fold range of initial concentrations reached a 14-fold range of concentrations after 7 days. Data are average over three repeated experiments (Figure S1D).

(C) Ratio of initial concentration range to final concentration range in the experiments shown in (A and B). Wild-type cells show much less sensitivity to initial cell numbers than cells deleted for the IL-2 gene.

(D) Coefficient of variation (CV) calculated on the last day of experiments. The CV indicates the convergence of cell cultures on the last day. Wild-type cells show a CV ~2.5-fold lower than cells deleted for the IL-2 gene.

The error bars in (C and D) indicate the SEM across experimental repeats. See also Figures S1 and S2; Table S2.

group, we chose to focus our study on these activated cells. Similar results were also obtained by analysis of the entire cell population (Figure S1B).

We performed the experiment at ten different initial cell levels. At the beginning of the culture, cell concentration spanned a range of 31.9 ± 2.4-fold (average ± SEM of 4 experimental repeats; Figures S1C and S1D). At the end of the process (day 8), the concentration range was reduced to 2.2 ± 0.5-fold (Figure 2A). Therefore, the cell concentration range decreased about 15-fold (Figure 2C).

We noted that cell levels were not limited by the carrying capacity of the cell culture, as shown by repeating the experiment while removing the cells from the TCR stimulus at day 4 but leaving them in the same growth medium. In this case, cells reached cell concentrations that were 2- to 3-fold higher than the homeostatic level (Figure 2A, red dashed line). Similarly higher cell levels were obtained when stimulating T cells from TCR transgenic mice with splenic dendritic cells presenting the corresponding cognate antigen (Figure S1E). We also found that cell expansion is not limited by a depletion of resources. Experiments where we replenished the medium at days 3 or 4 or where we diluted cell numbers at day 3 all led to a similar homeostatic level.

At very low total initial cell concentrations, below ~320 activated cells/ml at day 1 (the "threshold level"), we found that, without exogenous IL-2, cell concentrations decayed to zero within 5 days (Figure 2A, inset). When the initial concentration was higher than this threshold, cell concentrations approached an approximately fixed, initial condition-independent level that was ~17-fold higher than the threshold. Hereafter, we use the term "homeostasis" for the tendency of cells to reach an initial level independent concentration. We use the term OFF-state for the fact that low initial cell concentrations decay toward zero concentration. To summarize these findings, we observed homeostasis for high enough initial cell levels and an OFF-state for low initial cell levels.

Homeostasis Is Dependent on IL-2 Production by Cells

We next wanted to test whether IL-2 secretion by cells plays a role in the observed homeostasis. For this purpose, we used mouse CD4⁺ T cells deleted for the *il-2* gene (IL-2 knockout [KO]) (Naramura et al., 1998). The cells were cultured in medium with and without external IL-2. We found that IL-2 KO cells cultured without external IL-2 in the medium showed very limited initial proliferation and died within 3 days from the beginning of the experiment (Figure S1F). Addition of 20 ng/ml IL-2 to the culture resulted in cell growth. However, cell levels at the end of the experiment still showed dependence on the initial conditions. A much smaller fold reduction of the initial range occurred than in wild-type cells. The initial range spanned by cells was 39.8 ± 6.8 and was reduced after 7 days to only 13.8 ± 5.5 (Figure 2B). In other words, the spanned range of IL-2 KO cells decreased less than 3-fold (Figure 2C) compared with an approximately 15-fold decrease in wild-type cells. Similar results were obtained for IL-2 KO cells cultured in the presence of lower (6 ng/ml) and higher (80 ng/ml) doses of external IL-2 (Figures S2A–S2C). These measurements suggest that IL-2 secretion by cells plays an important role in the homeostasis of CD4⁺ T cells in our in vitro system.

To better characterize the mechanisms involved, we next measured IL-2 dynamics and their dependence on initial cell

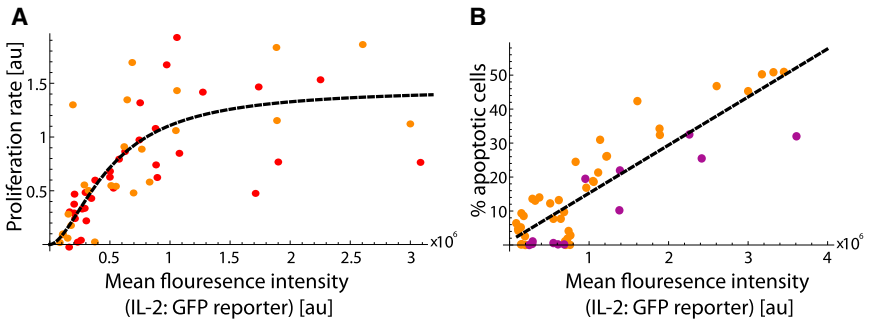

Figure 3. Proliferation and Death Rates Increase with IL-2 Production by Cells: The Former Cooperatively and the Latter Linearly

(A) Average proliferation rate measured by CFSE analysis (see Experimental Procedures) as a function of IL-2 reporter GFP fluorescence. Data from two experiments are shown (orange and red). au, arbitrary units.

(B) Average percentage of apoptotic cells measured by an Annexin assay as a function of IL-2 reporter GFP fluorescence. Data are from the same experiment as in (A) (orange) and another repeated experiment (purple). The minimal value of each data set (point with minimal percentage of stained cells) was subtracted to account for the offset between experiments because of fluorescence background differences and gating biases (Figure S3H). Lines are best fit to Hill functions, showing a Hill coefficient of n = 1.7 ± 0.5 for proliferation (A) (Figure S3G) and n = 1 ± 0.1 for the death rate (B) (Figure S3H).

See also Figure S3.

concentration. IL-2 levels in the cell culture medium were measured by ELISA. In addition, we evaluated IL-2 promoter activity using a GFP reporter (see Experimental Procedures). We found, using both methods, that IL-2 levels increased and then declined and that IL-2 peak height and pulse duration are anti-correlated with initial cell levels (Figures S2D–S2H). Smaller initial cell levels gave rise to longer pulse duration and a higher peak height, resulting in an overall larger pulse of IL-2. A similar dependence of IL-2 pulse level and peak timing on initial cell numbers was observed recently using T cell stimulation with antigen-presenting dendritic cells (Tkach et al., 2014).

IL-2 Signaling Has a Paradoxical Role Supporting Both Cell Proliferation and Cell Death

We next asked how IL-2 affects cell proliferation and death rates. Proliferation was measured by staining naive $CD4^+$ T cells with CFSE, a cell staining dye whose concentration drops by a factor of two with every cell division. This allowed the accurate determination of cell proliferation rate dynamics (see Experimental Procedures). To measure the death rate, we stained samples of cells from the same experiment with Annexin V, a marker for apoptosis that indicates the fraction of dying cells (see Figures S3A–S3C for representative scatter plots). Each experiment provided 25–40 data points composed of 7–10 initial cell concentrations measured across 4 or 5 days of experiments. Each data point contains three measurables: mean IL-2 GFP reporter levels, proliferation rate (evaluated from CFSE staining), and death rate (evaluated from Annexin staining).

We found that the proliferation and death rates were positively correlated with IL-2 reporter activity (see Experimental Procedures). The proliferation rate correlated with the IL-2 reporter level in a cooperative way, well described by an effective Hill coefficient n = 1.7 + –0.5 (Figure 3A; Figures S3D–S3G). The death rate was found to be linearly dependent on IL-2 reporter levels, n = 1 + −0.1 (Figure 3B; Figure S3H). We noted that the death rate was weakly dependent on confluency effects because cell concentrations were far from the carrying capacity of the wells. Additionally, we found no correlation between the fraction of Annexin V positive cells and the number of cell divisions in our experiments (data not shown). These observations suggest that IL-2 has a paradoxical role in the expansion process of $CD4^+$ T cells under these conditions, enhancing, at the same time, the proliferation and death rates (Lenardo, 1991; Li et al., 2001; Refaeli et al., 1998; Smith, 1988; Wang et al., 1996).

A Simple Mathematical Model Captures IL-2-Dependent Cell Dynamics

To understand how paradoxical signaling by IL-2 can lead to homeostasis, we studied a mathematical model of this system (Hart et al., 2012). The model assumes that $CD4^+$ T cells secrete IL-2 and also remove IL-2 from the medium by endocytosis. IL-2 increases both the proliferation and death rate. IL-2 can also be supplied externally and is degraded at a slow rate (the IL-2 degradation rate is taken to be 2 orders of magnitude smaller than the endocytosis rate, in accord with previous studies [Fujii et al., 1986; Molina-París, 2011]). The model equations are given in Figure 4A (see Supplemental Information for details). The secretion rate of IL-2 per cell was assumed to be constant. Endocytosis of IL-2 was assumed to be a cooperative increasing function of IL-2 (with a Hill coefficient of 2) because IL-2 receptor levels (IL2-Rα or CD25) increase cooperatively with IL-2 levels (Depper et al., 1985; Waysbort et al., 2013). Similar results were obtained for a Michaelis-Menten dependency of endocytosis on IL-2 levels.

In a previous study, we showed that this set of equations produces a robust final concentration of cells that is independent of initial cell levels (Hart et al., 2012). To test the model's ability to capture $CD4^+$ T cells dynamics in the presence of IL-2, we simulated the model using the measured experimental dependence of proliferation and death on IL-2: a proliferation rate that rises cooperatively with a Hill coefficient of 2 and a death rate that is linear in IL-2 (Figures 3A and 3B, respectively). The model has two stable steady-state solutions, ON-state and OFF-state, that originate from the combination of two feedback loops, a positive feedback loop where IL-2 drives proliferation and a negative feedback loop where it drives cell death. Homeostasis can be explained intuitively as the result of the negative feedback loop on cell number, where the system has a fixed point at high cell levels. Above this level, cell death dominates, and below it, proliferation dominates, resulting in a stable fixed point (the ON-state) that is reached for a wide range of initial cell concentrations. The positive feedback through which IL-2 increases the proliferation rate creates a threshold level below which resides a

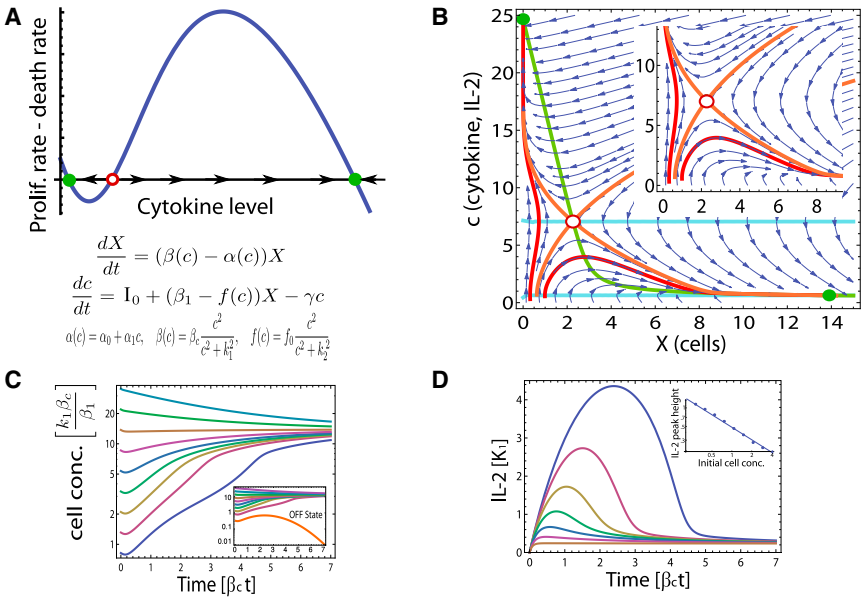

Figure 4. A Simple Mathematical Model in which IL-2 Increases Both the Proliferation and Death Rates Captures the Observed Cell Homeostasis and IL-2 Dynamics

(A) Model differential equations in which we used the present experimental results to describe the effects of IL-2 on proliferation ($\beta(c)$) and death ($\alpha(c)$) as cooperative and linear, respectively. I_0 is a possible external source/sink of cytokine c. β_1 is the secretion rate of the cytokine by the cells. γ is the degradation rate of c and is assumed to be small. The uptake rate by the cells is denoted by $f(c)$, where endocytosis was assumed to be cooperative because IL-2 levels were shown to increase IL-2 receptor levels cooperatively (similar results are found when the uptake rate has a Michaelis-Menten dependence on IL-2 levels). The proliferation minus death rate as a function of cytokine crosses zero three times, resulting in two stable fixed points (green filled circles) and one unstable fixed point (red empty circle). Arrows on the x axis show the flow toward the stable fixed points.

(B) A phase diagram of the simulated model shows two fixed points, one at low cell concentration (OFF-state, upper left green filled circle) and another at medium cell concentration (ON-state, lower right green filled circle). The green solid line is the nullcline for $X'(t) = 0$, and light blue lines are the nullclines for $c'(t) = 0$. Full green and empty red points indicate stable and unstable fixed points of the model, respectively. Blue arrows show the flow in the phase diagram. Red lines show two specific trajectories of initial cell and IL-2 concentrations near the separatrix, where one trajectory (left) goes to the OFF-state and the other (right) goes to the ON-state. The inset shows magnification around the unstable point.

(C) Simulated dynamics of the model show that a fixed final cell concentration is reached for a wide range of initial cell concentrations (cell conc.). Very low initial concentrations result in a decline to a vanishing cell population (inset, orange line). Compare this with the experimental results in Figure 2A.

(D) Simulated IL-2 levels show pulse-like dynamics. The inset shows that the pulse peak height is inversely correlated with initial cell levels, with a power law exponent of -0.67 ± 0.08. Compare this with the experimental results in Figures S2D–S2G. All units in (C and D) are in dimensionless numbers, given by the dimensionless parameter combinations indicated on the axes, and, therefore, represent a qualitative agreement with the experimental measurements. Best fit parameters for the dimensionless model are $a_1 = I_0/(k_1\ \beta_c) = 10$, $a_2 = \gamma/\beta_c = 1.2$, $a_3 = f_0/\beta_c = 9.1$, $a_4 = \alpha_0/\beta_c = 0.12$, $a_5 = \alpha_1 k_1/\beta_c = 0.1$. The model is robust to changes in parameter values, as indicated by the fold change range over which each of these best fit parameters can be varied while changing the error function values by less than 50%: $a_{1,max}/a_{1,min} = 1.6$, $a_{2,max}/a_{2,min} = 6.5$, $a_{3,max}/a_{3,min} = 1.5$, $a_{4,max}/a_{4,min} = 2.6$, $a_{5,max}/a_{5,min} = 3.6$.

See also Figure S4.

second fixed point (the OFF-state), which is reached when initial cell levels are very low (Figures 4A and 4B).

The five parameters of the dimensionless model were fit to give the best agreement with the experimental data of wild-type (WT) cell level dynamics and measured IL-2 levels. The calculated model dynamics are in good agreement with the measured dynamics of both cell levels (Figure 4C) and IL-2 levels (Figure 4D). In particular, the measured dependencies of the proliferation and death rates on IL-2 levels reproduced in the model homeostasis of final cell levels, existence of an OFF-state, and pulsed dynamics of IL-2. Moreover, the model reproduced the observed negative correlation between IL-2 peak height and initial cell levels in which the peak height scales as $X_0^{-0.67 \pm 0.08}$ (Figure 4D, inset), which is similar to the observed experimental behavior (Figure S2). It should be noted that the model produced qualitatively similar behavior over a wide range of parameters (Figure S4).

Final Levels of IL-2-Deficient Cells and Bcl-2 Expression Depend Nonmonotonically on External IL-2 Levels

If IL-2 levels indeed have a paradoxical role, enhancing both proliferation and death, one would expect that, for each initial cell concentration, only a small range of IL-2 levels would produce a valid expansion process. Outside of this small range, IL-2 levels are too low to support expansion or too high, causing increased cell death. To check this hypothesis, we solved the model for the case of IL-2-deficient cells that were cultured in the presence of different levels of external IL-2. We simulated the model using parameters extracted from the fit, as mentioned above, but set the secretion rate of IL-2 by the cells to zero and added an external source of IL-2. The simulation predicted that final cell levels would depend on external IL-2 concentration in a nonmonotonous way. Final cell levels should be low for both low and high IL-2 levels and should be maximal in an intermediate range of external IL-2 levels (Figure 5A).

To test this prediction of the model experimentally, we measured the expansion process of a fixed amount of $CD4^+$ T cells deleted for the *il-2* gene with different external IL-2 levels in the medium (Figures 5B; Figure S5). IL-2 levels spanned 4 orders of magnitude, ranging from 0.03-500 ng/ml. We found that, for low external IL-2 levels, cell levels decayed rapidly to a very low concentration of cells (Figure 5B, red lines). High levels of external IL-2 also resulted in a 2-fold decrease in cell levels (Figure 5B, blue lines), indicating a change in the balance between proliferation and apoptosis. Only a small range of IL-2 concentrations (ranging between 2-6 ng/ml) produced an expansion of

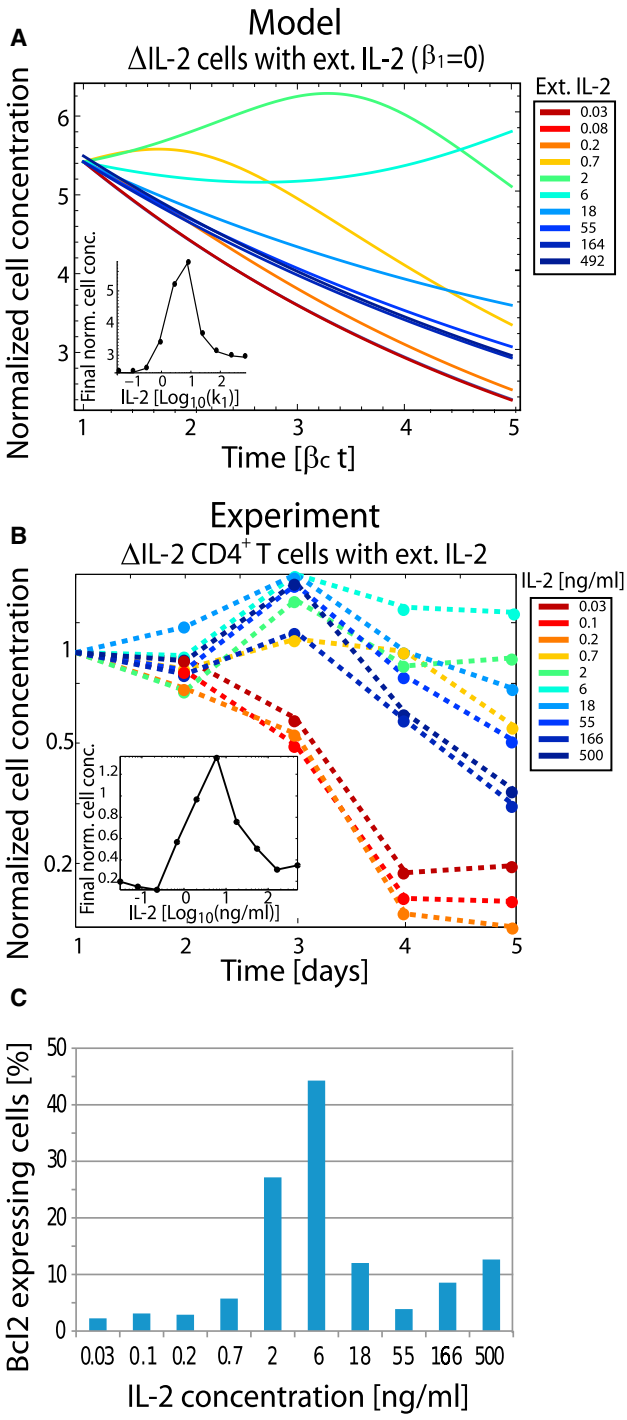

Figure 5. Without Endogenous Production of IL-2, Cells Require a Specific Concentration of External IL-2 to Reach High Cell Numbers; at This Concentration, Antiapoptotic Bcl2 Is Induced

(A) Model of cells that do not produce IL-2 (IL-2 deleted cells) shows high cell numbers only in a limited range of external IL-2 (ext. IL-2) concentrations. External IL-2 concentrations are in K_1 units and are increased 3-fold from one curve to another (see legend). Compare this with the experimental results in Figure 5B.

(B) Measured cell concentration dynamics of $CD4^+$ T cells deleted for the IL-2 gene at different levels of IL-2 supplied to the growth medium at culture starting time. The initial cell concentration corresponds to 5,600 ± 200 activated cells/ml at day 1. Data were normalized to the initial concentration in each experiment. The insets (A and B) show that the final cell number (day 5) is highest at intermediate IL-2 concentrations (2–6 ng/ml).

(C) Fraction of cells expressing the antiapoptotic Bcl-2 protein measured by anti-Bcl-2 antibody staining and flow cytometry. The fraction of cells expressing Bcl-2 is highest at an intermediate level of IL-2 (2–6 ng/ml).

See also Figure S5.

cells to final levels that are similar to, or higher than, the initial levels (Figure 5B, turquoise green lines). As predicted by the model, the final cell levels depended on IL-2 concentration non-monotonically, reaching a peak at intermediate IL-2 levels and decreasing for both low and high external IL-2 levels (compare Figure 5A inset and Figure 5B inset).

Previous studies (Dai et al., 1999; Li et al., 2001; Rochman et al., 2009) have suggested that IL-2 increases apoptosis of $CD4^+$ T cells by affecting Bcl-2 levels through the IL-2 receptor γ-subunit. Dai et al. (1999) demonstrated that exogenous IL-2 downregulates IL-2 receptor γ chain (γc) expression in vitro and that endogenous IL-2 limits γc expression on activated $CD8^+$ T cells in vitro and in vivo. Cytokines that do not promote cell death (IL-4, IL-7, and IL-15, which use the same γc) did not influence γc expression. They also demonstrated that blocking the common cytokine receptor γ chain prevented Bcl-2 induction and, by this, augmented cell death. To test the effect of IL-2 on Bcl-2 levels in our system, we used a Bcl-2 antibody to measure Bcl-2 levels in cells from the same experiments (IL-2 KO cells grown at different IL-2 levels). We found that the Bcl-2 level in the cells was low for both high and low external IL-2 levels. In contrast, Bcl-2 levels were high for intermediate levels of external IL-2 (2–6 ng/ml, Figure 5C), correlating well with the observed dependence of cell expansion on IL-2 levels (Figure 5B, inset).

The Model Correctly Predicts that Cell Dilution Can Switch the System from Homeostasis to the OFF-State

Another interesting prediction of the model is that the system can be switched from the homeostatic to the OFF-state by the dilution of cell concentration. The paradoxical role of IL-2 implies that a similar level of IL-2 can be either proproliferative or lead to extinction, depending on the current cell concentration and cell state in terms of IL-2 production and consumption rates. As an example, if one takes cells during the expansion phase and dilutes them to a low enough concentration, one is predicted to shift the cell trajectory from reaching the homeostasis level, the ON-state, to extinction, the OFF-state. This occurs because IL-2 levels are too high for the new low amount of cells and, therefore, lead to cell death. Figure 6A shows a schematic of this kind of transition between points 1 and 2 in the phase space of cell concentration and IL-2 levels. On the other hand, if the level of cells is high enough above the critical line in this phase space (separatrix, orange lines), then cells will recover after dilution and attain the ON-state homeostatic level (Figure 6A, transition between points 3 and 4).

We tested this prediction experimentally by culturing cells at different initial concentrations and diluting their concentration 3-fold at day 3, keeping medium conditions the same. As

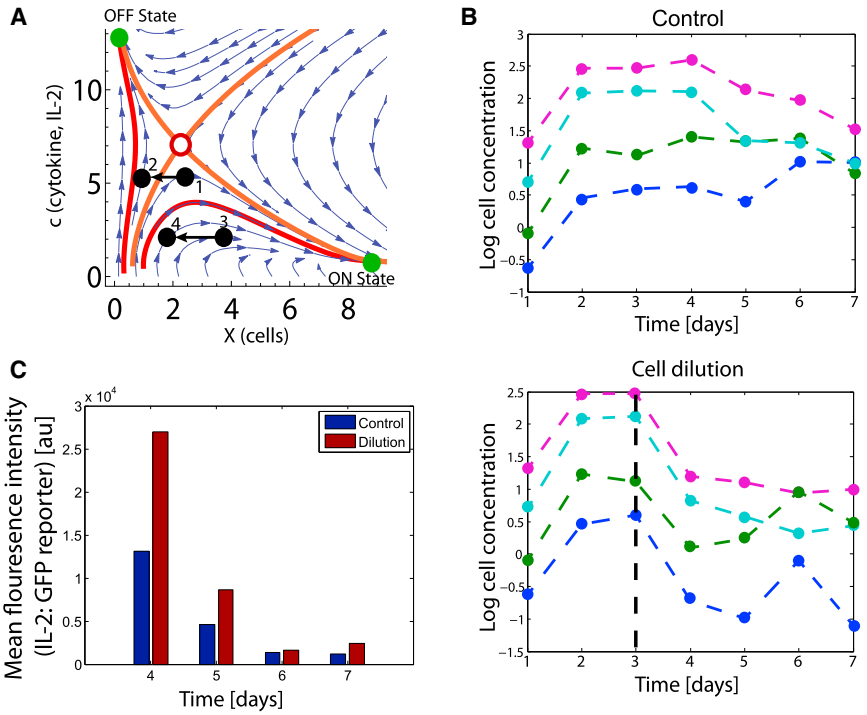

Figure 6. Dilution of Cells while Proliferating Can Transfer Their Fate to the OFF-State

(A) A schematic representation of transforming cells from reaching the homeostatic ON-state to reaching the OFF-state. When cell levels are changed during the expansion process, the cells' final fate can change. When cells are diluted from state 1 to state 2, IL-2 levels are too high relative to their new concentration, and therefore, they decay to extinction, the OFF-state. On the other hand, the same level of dilution, when cell concentration is high enough, will not cause change of cell fate, as exemplified by the dilution from state 3 to state 4. Note that IL-2 levels rise when cell fate is changed to the OFF-state.

(B) Experimental test of cell dilution. Top panel. in a control experiment, cultured $CD4^+$ T cells at different initial concentrations reach the homeostasis level. Bottom panel, cells of the same initial levels are diluted 3-fold on day 3 (dashed black line). The lower concentration culture (blue) died off to extinction (the OFF-state), whereas the cultures with higher initial cell concentrations reach homeostasis level.

(C) IL-2 GFP fluorescence levels are twice as high when the cell culture is going to the OFF-state compared with their levels in the control experiment (no dilution) when they reach the homeostatic ON-state level.

See also Figure S6, Table S1.

predicted by the model, high cell concentrations reached the homeostatic level even after dilution, whereas cells with an initial low concentration showed extinction after the dilution (Figure 6B). Specifically, cells seeded at a low concentration (about 1,300 activated cells/ml at day 1) reached homeostasis when not diluted but reached extinction when diluted after 3 days, when dilution brought them back to roughly their initial level. Therefore, extinction does not merely reflect cell levels but depends on the altered state of the medium in the 3 days prior to dilution (Figures 6B and 6C).

The model further predicts that, after the dilution, IL-2 production should be higher in the cell cultures going to extinction (Figure 6A, red path upward from point 2) compared with the cultures going to homeostasis (Figure 6A, red path going right from point 4). We measured IL-2 GFP fluorescence of all cultures every day after dilution. We found that the IL-2 GFP level of the culture going to extinction was at least 3-fold higher on day 4 (1 day after dilution) compared with the other (homeostatic) cultures (Figure S6). Furthermore, the IL-2 GFP levels of the OFF-state culture was twice as high compared with the same culture (same initial cell level) in a control experiment (no dilution) when it reached the homeostatic level (Figure 6C; Table S1). In the other cultures, which reached homeostasis after cell dilution, average IL-2 GFP fluorescence levels were similar to those of the undiluted control (Table S1).

Separating the Functions of the Paradoxical Signaling Molecule into Two Separate Monofunctional Molecules Hampers Robustness

Lastly, we ask the following question: why is a single molecule with two antagonistic functions better suited for achieving homeostasis than two different molecules, each endowed with one of the two functions? To answer this question, we modified our model of Figure 4 to include two signaling molecules: one that causes cells to increase their proliferation rate in a cooperative manner and a second that increases the cell death rate linearly (Figure 7A). The cells secrete and take up both molecules. In general, we found that, when the circuit contains two signaling molecules, the intrinsic integral feedback mechanism that keeps homeostasis of cell numbers breaks down. Therefore, the circuit dynamic behavior depends much more sensitively on its parameters.

As a specific example for this sensitivity, we calculated the steady states of the two-molecule system for a case in which the molecules are supplied by external sources in addition to their secretion by the cells. We found that there was only a very limited range of parameters for which the cell circuit can achieve both a homeostatic ON-state and an OFF-state. For most of the parameter range, the cell circuit is either always ON or always OFF (Figure 7B; Figure S7). In contrast, the model with one paradoxical signaling molecule achieves this property for a wide range of values of the external source strength (see Extended Experimental Procedures). These results are not restricted to the particular model used here but are an inherent property of the break of paradoxical signaling into two distinct monofunctional signaling molecules.

To understand why a paradoxical component is more robust, consider that the homeostasis and OFF-state depend on three intersection points of the death and proliferation curves (Figure S7). A paradoxical component constrains these curves to vary in a coordinated manner because they depend on the same molecule keeping the three intersection points robust. If

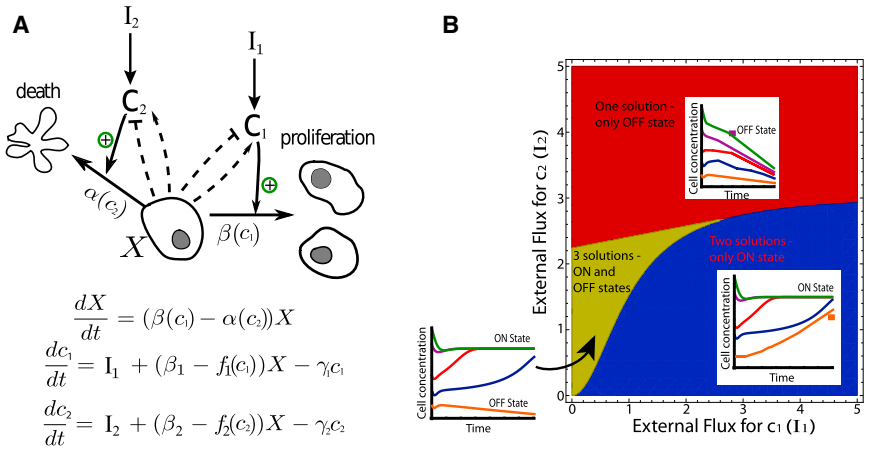

Figure 7. Separating the Two Paradoxical Roles into Two Signaling Molecules Hampers Robustness

(A) Schematic and equations of a model with two signaling molecules carrying the roles of proliferation (c_1) and apoptosis (c_2). $I_{1,2}$ are external sources of the signaling molecules. $\beta_{1,2}$ are the secretion rates of the signaling molecules by the cells. $f_1(c_1)$, $f_2(c_2)$ are the uptake rates of the signaling molecules by the cells (cooperatively dependent on the molecules). $\gamma_{1,2}$ are the degradation rates of c_1 and c_2 and are assumed to be small. $\beta(c_1)$ is the proliferation rate, which depends cooperatively on c_1 levels. $\alpha(c_2)$ is the death rate, which depends linearly on c_2 levels.

(B) Phase diagram of the possible steady-state solutions achieved depending on the relative levels of I_1 and I_2, the signaling molecules external sources. There is a small parameter range where the system achieves both an ON-state and an OFF-state (yellow region). A deviation from this parameter range causes the system to be either in a constant ON-state (blue region) or in a constant OFF-state (red region).

See also Figure S7.

each curve depended, instead, on a different monofunctional molecule, then the two curves would vary independently with external supply and removal of these molecules, and the crossing points can vanish easily (Figure S7).

DISCUSSION

Our results demonstrate a design principle for cell circuits where paradoxical signaling by a secreted molecule generates a specific desired biological function: a system with both a homeostatic ON-state and an OFF-state. Our mathematical model captures many aspects of the system's dynamic behavior over a large range of parameter values. It also provides unintuitive testable predictions, such as an inverse relation between initial cell numbers and the amplitude of the IL-2 pulse (Figure 4D; Figure S2), a nonmonotonic dependence of final cell numbers on levels of external IL-2 (Figure 5), and a decay to an OFF-state when cells are diluted while maintaining the level of IL-2 in the medium (Figure 6). Therefore, the model and experiments provide a framework for a better understanding of the dynamic coupling between cell numbers and cytokine levels and the ways in which they are influenced by various perturbations.

How can IL-2 secretion by cells stabilize cell numbers? Because the cytokine increases the death rate linearly but the proliferation rate cooperatively, the difference between the two rates is negative (the death rate is higher than the proliferation rate) at both low and high cytokine levels and is positive in an intermediate range of cytokine levels (Figure 4A). Hence, the system has two stable fixed points, the OFF-state and the homeostatic state, and an intermediate unstable point at the threshold level. Above the threshold, the cells self-tune to reach a concentration at which the IL-2 level is such that proliferation equals death. This homeostatic point is stable. If the cell concentration rises above the fixed point, death predominates, and cell numbers decrease. If cells drop below the fixed point, proliferation dominates, and cell numbers increase. As a result, deviations from the fixed point concentration are corrected, and the fixed point is stable. This situation holds true for a large class of death and proliferation rate dynamics, as shown previously (Hart et al., 2012). Below the threshold, the death rate predominates, and cell levels decline to the OFF-state.

We showed that we can change the cells' fate from reaching the homeostatic level (ON-state) to extinction (OFF-state) by diluting cell levels while keeping IL-2 levels constant. This is an example of experimentally crossing the separatrix (threshold) between the two states (Figure 6). Although, in the mathematical model, the threshold is sharp and unique, determining its experimental level is challenging. For a general case of paradoxical signaling, changing proliferation and death rate dependencies on the signaling molecule can bring the threshold closer to the OFF-state, thus creating a system that could be driven by noise.

The use of an in vitro system allowed for a controlled experimental model in which cell numbers and cytokine levels could be manipulated and quantitatively followed dynamically. This allowed for accurate testing of model predictions by exploring the system's phase space in different situations. The initial cell levels we used cover the expected physiological range for antigen-specific T cells ($\sim 10^4$–10^5 T cells/ml specific for a given complex pathogen within a lymph node). However, the in vitro system has some differences when compared with the situation in vivo. For example, we used persistent stimulation of the T cells, whereas in vivo T cell stimulation is dynamic. The persistent stimulation may restrict cell expansion, which is lower in our in vitro system ($\sim$10-fold) compared with in vivo measurements (which typically show $\sim$100-fold expansion or higher). In general, the in vivo situation is more complex because T cells can secrete and respond to several cytokines and are affected by other cells in their environment. Therefore, the cell circuit described here is embedded within a larger network of interacting cells. Such networks can involve other layers of regulation and redundancies, which obscure the investigation of the underlying design principles. We suggest that, by separating composite circuits into tractable, simpler building blocks, it may be possible to decipher the function of cell circuits with growing complexity.

The finding of homeostasis is in line with previous adoptive transfer experiments of T cells in mice. These experiments showed that effector cell levels are very weakly dependent on initial precursor levels both in $CD4^+$ and $CD8^+$ T cells (Badovinac et al., 2007; Quiel et al., 2011; Whitmire et al., 2006, 2008; Williams et al., 2008). For example, Whitmire et al. (2006) used an adoptive transfer experiment to measure expansion and proliferation of transferred and endogenous cells. Interestingly, across a range of 3 orders of magnitude of precursor frequency, the total expansion of cells changed by about half an order of magnitude (see Figure 2B in Whitmire et al., 2006). Several studies suggest that IL-2 is dispensable for primary T cell expansion in vivo (Liao et al., 2013; Malek, 2008). For example, a study by Quiel et al. (2011) showed that neither the external provision of IL-2 nor the inability of the stimulated T cells to produce IL-2 had an effect on their antigen-driven expansion in vivo. These results convey the complexities of T cell proliferative homeostasis in vivo, and further work is required to understand and model the intricacies of the different layers of regulation at play, for example by other cytokines with overlapping activities.

In our model and experiment, we consider the average behavior of the cell population. Future work can extend this study to describe the response of heterogeneous cell populations. For example, it is known that IL-2 is secreted only by a subpopulation of activated cells at a given time (Podtschaske et al., 2007; Waysbort et al., 2013), and the levels of IL-2 receptor also vary among cells, even when grown under the same conditions in vitro (Feinerman et al., 2010). Such heterogeneity may result in more complex behaviors, especially near bifurcation (threshold) points where sensitivity to variability is increased. Experimentally, such studies will require following individual cell responses dynamically, which can be done using live cell imaging (Day et al., 2009; Zaretsky et al., 2012). Another avenue for future research is to incorporate dynamic stimulation into the model and investigate its effects theoretically and experimentally.

A natural question that arises is as follows: what are the benefits of having two opposite functions carried by the same molecule rather than having two molecules, each with a specific role? Extracellular signaling molecules are affected by the microenvironment. Neighboring cells may secrete or consume these molecules with varying rates, therefore affecting their levels. If two molecules carry opposing functions, changes in the composition or state of the neighboring cells will generally change the relative levels of the two signaling molecules. As a result, the cell circuit function loses its decoupling from the environment. Instead of responding to their own cell level, cells respond to environmental cues. For example, we found that having two separate signaling molecules that are made by the cells but are also supplied by the environment at different rates disrupted the topology of phase space. For most parameter ranges, the two-molecule circuit either has only an OFF-state or only an ON-state (Figure 7). In contrast, having the two functions carried by the same molecule allows the circuit to have both states in a wide range of parameters. Supply of this paradoxical molecule from the outside increases both the death and proliferation rates but keeps their ratio relatively unaffected. External supply can affect the precise value of the homeostatic level but cannot abolish the qualitative phenomenon of homeostasis with an OFF-state. Therefore, we suggest that paradoxical signaling is important for robust function of the cell circuit and for its relative decoupling from the environment because changes in the cell parameters and in the environment affect both functions (proliferation and death) in a coordinated manner.

Paradoxical signaling appears to be widespread among immune system cytokines (Ashcroft, 1999; Busse et al., 2010; Feinerman et al., 2010; Li and Flavell, 2008; McGeachy and Cua, 2008; Sakaguchi, 2004; Villarino et al., 2006). There is also evidence for paradoxical signaling by secreted molecules in other systems in which a biomolecule affects both the proliferation and death of interacting cells (Dadon et al., 2012). It would be interesting to study whether such paradoxical effects can also provide homeostasis in these systems. A theoretical analysis suggests that, in other contexts, paradoxical components can provide other systems-level functions, such as differentiation processes that are independent of precursor cell numbers (Hart et al., 2012). Paradoxical signaling may, therefore, play a role in providing cell circuits with desirable dynamical properties that are resistant to environmental fluctuations.

EXPERIMENTAL PROCEDURES

Mice

Female C57BL/6 mice were obtained from Harlan Laboratories. IL-2-GFP knockin mice (Naramura et al., 1998) were provided by Prof. Ron Schwartz, National Institutes of Health. IL-2 reporter mice (Yui et al., 2004) were provided by Prof. Ellen Rothenberg, California Institute of Technology. All mice were housed at the Weizmann Institute in compliance with national and international regulations.

Cell Culture

Naive $CD4^+$ T cells were purified from splenocytes by magnetic bead separation ($CD4^+CD62L^+$ MACS, Miltenyi Biotec). Cells were stained with CFSE, diluted to defined initial cell concentrations, and cultured in complete RPMI 1640 medium at 37°C. The cells were stimulated using plates coated with anti-CD3 (1 μg/ml) and anti-CD28 (3 μg/ml) for 7–8 days. Eight different combinations of anti-CD3 and anti-CD28 doses showed no effect on homeostasis, except at very low stimulation levels (Table S2). Every day, a sample of cells was taken for counting and measuring CFSE levels and cell viability by flow cytometry. GFP levels for reporter strains were also measured by flow cytometry.

CFSE Staining

Freshly purified T cells were resuspended in PBS at 10^7 cells/ml and incubated with 1 μM CFSE (Invitrogen) for 10 min at 37°C. Cells were washed and resuspended in culture medium at the indicated cell concentrations.

Flow Cytometry

Where indicated, cells were stained with Annexin V Pacific blue (BioLegend) for 15 min at room temperature. Where indicated, cells were also stained with anti Bcl-2 FITC antibodies. Cells were then stained with 7-amino actinomycin D (7-AAD, BioLegend) to distinguish between live and dead cells. Flow cytometry analysis was performed using BD LSRII (BD Biosciences).Viable lymphocytes were gated based on forward/side scatter and negative 7-AAD staining. Cell concentrations were calculated according to a constant flow rate of 1.5 μl/s using a linear fit of the number of cells per unit time in the flow cytometry data.

ELISA on Beads

Quantitative evaluation of IL-2 levels in the supernatant was done using an extension of the ELISA assay with spectrally distinguishable beads (Sphero-tech) as the solid phase. Primary antibodies were covalently linked to the beads, which were incubated simultaneously with the supernatant and

secondary biotinylated antibodies for 2 hr, washed, and stained with streptavidin-phycoerythrin secondary antibodies. The bead fluorescence level was compared to a standard curve to quantitate the IL-2 level. Beads were analyzed using BD LSRII.

Data Analysis

CFSE histograms were fitted to a sum of Gaussians centered at expected division levels (Banks et al., 2011a, 2011b; Deenick et al., 2003). The proliferation index was calculated as the weighted average number of divisions where the weights are the Gaussian amplitudes. The proliferation rate was calculated as the change between days in the proliferation index, which correlates with the proliferation rate term that is used in the model ($\beta(c)$).

For analysis of cell death using Annexin V staining, all data points at different days from every initial cell concentration were collected. To evaluate the death probability at each IL-2 level, we extracted the percentage of Annexin V positive cells from flow cytometry data. This is a measure of cell death rate because it captures cells at early stages of apoptosis, whereas cells at later stages of apoptosis would stain as dead cells and also have a different forward scatter-side scatter (FSC-SSC) pattern. Therefore, the percentage of Annexin V^+ cells (gated on FSC-SSC and live) at a given time point correlates with the death rate term that is used in the model, ($\alpha(c)$). For the analysis of Figure 3, proliferation rate values, death rate values, and IL2-GFP MFI values were smoothed with a time window of 2 points. The experiment used for the purple data in Figure 3B included fewer time points than the one used for the orange data points. Data from cultures with extreme cell concentrations (high and low) were not used for this analysis if the fit to the CFSE data was not reliable.

Fit of the dimensionless model equations to experimental data was done using Mathematica 8.0, where model parameters (Figure 4) were fit to match cell concentration data and IL-2 levels, which were normalized to their initial levels. Further details about the model are given in the Supplemental Information.

SUPPLEMENTAL INFORMATION

Supplemental Information includes Extended Experimental Procedures, seven figures, and two tables and can be found with this article online at http://dx.doi.org/10.1016/j.cell.2014.07.033.

AUTHOR CONTRIBUTIONS

Y.H., S.R.Z., and Y.E.A. conceived the main hypotheses for the project. Y.H., S.R.Z., Y.E.A., and N.F. designed the experiments. S.R.Z., Y.E.A., and I.Z. performed the experiments. Y.H., S.R.Z., Y.E.A., and A.E.M. analyzed the experimental data. Y.H., A.E.M., and U.A. developed the mathematical models. Y.H. and A.E.M. performed the mathematical and numerical analysis. Y.H., S.R.Z., U.A., and N.F. wrote the paper. N.F. supervised the project.

ACKNOWLEDGMENTS

This research was supported by grants from the Israeli Science Foundation, The Human Frontier Science Program, and the European Research Council under the European Union's 7th Framework Programme (ERC Grant agreement 249919) (to U.A.). This research was also supported by a grant from the I-CORE Program of the Planning and Budgeting Committee and the Israel Science Foundation (to N.F.). U.A. is the incumbent of the Abisch-Frenkel Professorial Chair. N.F. is the incumbent of the Pauline Recanati Career Development Chair of Immunology. Y.H. wishes to thank Naama Barkai for fruitful discussions.

Received: July 11, 2013
Revised: March 10, 2014
Accepted: July 10, 2014
Published: August 28, 2014

REFERENCES

Ashcroft, G.S. (1999). Bidirectional regulation of macrophage function by TGF-beta. Microbes Infect. *1*, 1275–1282.

Badovinac, V.P., Haring, J.S., and Harty, J.T. (2007). Initial T cell receptor transgenic cell precursor frequency dictates critical aspects of the CD8(+) T cell response to infection. Immunity *26*, 827–841.

Banks, H.T., Sutton, K.L., Thompson, W.C., Bocharov, G., Roose, D., Schenkel, T., and Meyerhans, A. (2011a). Estimation of cell proliferation dynamics using CFSE data. Bull. Math. Biol. *73*, 116–150.

Banks, H.T., Sutton, K.L., Thompson, W.C., Bocharov, G., Doumic, M., Schenkel, T., Argilaguet, J., Giest, S., Peligero, C., and Meyerhans, A. (2011b). A new model for the estimation of cell proliferation dynamics using CFSE data. J. Immunol. Methods *373*, 143–160.

Busse, D., de la Rosa, M., Hobiger, K., Thurley, K., Flossdorf, M., Scheffold, A., and Höfer, T. (2010). Competing feedback loops shape IL-2 signaling between helper and regulatory T lymphocytes in cellular microenvironments. Proc. Natl. Acad. Sci. USA *107*, 3058–3063.

Cantrell, D.A., and Smith, K.A. (1984). The interleukin-2 T-cell system: a new cell growth model. Science *224*, 1312–1316.

Dadon, D., Tornovsky-Babaey, S., Furth-Lavi, J., Ben-Zvi, D., Ziv, O., Schyr-Ben-Haroush, R., Stolovich-Rain, M., Hija, A., Porat, S., Granot, Z., et al. (2012). Glucose metabolism: key endogenous regulator of β-cell replication and survival. Diabetes Obes. Metab. *14* (*Suppl 3*), 101–108.

Dai, Z., Arakelov, A., Wagener, M., Konieczny, B.T., and Lakkis, F.G. (1999). The role of the common cytokine receptor γ-chain in regulating IL-2-dependent, activation-induced CD8+ T cell death. J. Immunol. *163*, 3131–3137.

Day, D., Pham, K., Ludford-Menting, M.J., Oliaro, J., Izon, D., Russell, S.M., and Gu, M. (2009). A method for prolonged imaging of motile lymphocytes. Immunol. Cell Biol. *87*, 154–158.

Deenick, E.K., Gett, A.V., and Hodgkin, P.D. (2003). Stochastic model of T cell proliferation: a calculus revealing IL-2 regulation of precursor frequencies, cell cycle time, and survival. J. Immunol. *170*, 4963–4972.

Depper, J.M., Leonard, W.J., Drogula, C., Krönke, M., Waldmann, T.A., and Greene, W.C. (1985). Interleukin 2 (IL-2) augments transcription of the IL-2 receptor gene. Proc. Natl. Acad. Sci. USA *82*, 4230–4234.

Eldar, A., Dorfman, R., Weiss, D., Ashe, H., Shilo, B.-Z., and Barkai, N. (2002). Robustness of the BMP morphogen gradient in Drosophila embryonic patterning. Nature *419*, 304–308.

Feinerman, O., Jentsch, G., Tkach, K.E., Coward, J.W., Hathorn, M.M., Sneddon, M.W., Emonet, T., Smith, K.A., and Altan-Bonnet, G. (2010). Single-cell quantification of IL-2 response by effector and regulatory T cells reveals critical plasticity in immune response. Mol. Syst. Biol. *6*, 437.

Fujii, M., Sugamura, K., Sano, K., Nakai, M., Sugita, K., and Hinuma, Y. (1986). High-affinity receptor-mediated internalization and degradation of interleukin 2 in human T cells. J. Exp. Med. *163*, 550–562.

Hart, Y., and Alon, U. (2013). The utility of paradoxical components in biological circuits. Mol. Cell *49*, 213–221.

Hart, Y., Antebi, Y.E., Mayo, A.E., Friedman, N., and Alon, U. (2012). Design principles of cell circuits with paradoxical components. Proc. Natl. Acad. Sci. USA *109*, 8346–8351.

Haskel-Ittah, M., Ben-Zvi, D., Branski-Arieli, M., Schejter, E.D., Shilo, B.-Z., and Barkai, N. (2012). Self-organized shuttling: generating sharp dorsoventral polarity in the early Drosophila embryo. Cell *150*, 1016–1028.

Lamaze, C., Dujeancourt, A., Baba, T., Lo, C.G., Benmerah, A., and Dautry-Varsat, A. (2001). Interleukin 2 receptors and detergent-resistant membrane domains define a clathrin-independent endocytic pathway. Mol. Cell *7*, 661–671.

Lan, R.Y., Selmi, C., and Gershwin, M.E. (2008). The regulatory, inflammatory, and T cell programming roles of interleukin-2 (IL-2). J. Autoimmun. *31*, 7–12.

Lenardo, M.J. (1991). Interleukin-2 programs mouse alpha beta T lymphocytes for apoptosis. Nature *353*, 858–861.

Li, M.O., and Flavell, R.A. (2008). Contextual regulation of inflammation: a duet by transforming growth factor-β and interleukin-10. Immunity *28*, 468–476.

Li, X.C., Demirci, G., Ferrari-Lacraz, S., Groves, C., Coyle, A., Malek, T.R., and Strom, T.B. (2001). IL-15 and IL-2: a matter of life and death for T cells in vivo. Nat. Med. *7*, 114–118.

Liao, W., Lin, J.-X., and Leonard, W.J. (2013). Interleukin-2 at the crossroads of effector responses, tolerance, and immunotherapy. Immunity *38*, 13–25.

Malek, T.R. (2008). The biology of interleukin-2. Annu. Rev. Immunol. *26*, 453–479.

McGeachy, M.J., and Cua, D.J. (2008). Th17 cell differentiation: the long and winding road. Immunity *28*, 445–453.

Molina-París, C. (2011). Mathematical Models and Immune Cell Biology (New York: Springer).

Naramura, M., Hu, R.J., and Gu, H. (1998). Mice with a fluorescent marker for interleukin 2 gene activation. Immunity *9*, 209–216.

Podtschaske, M., Benary, U., Zwinger, S., Höfer, T., Radbruch, A., and Baumgrass, R. (2007). Digital NFATc2 activation per cell transforms graded T cell receptor activation into an all-or-none IL-2 expression. PLoS ONE *2*, e935.

Quiel, J., Caucheteux, S., Laurence, A., Singh, N.J., Bocharov, G., Ben-Sasson, S.Z., Grossman, Z., and Paul, W.E. (2011). Antigen-stimulated CD4 T-cell expansion is inversely and log-linearly related to precursor number. Proc. Natl. Acad. Sci. USA *108*, 3312–3317.

Refaeli, Y., Van Parijs, L., London, C.A., Tschopp, J., and Abbas, A.K. (1998). Biochemical mechanisms of IL-2-regulated Fas-mediated T cell apoptosis. Immunity *8*, 615–623.

Rochman, Y., Spolski, R., and Leonard, W.J. (2009). New insights into the regulation of T cells by gamma(c) family cytokines. Nat. Rev. Immunol. *9*, 480–490.

Sakaguchi, S. (2004). Naturally arising CD4+ regulatory t cells for immunologic self-tolerance and negative control of immune responses. Annu. Rev. Immunol. *22*, 531–562.

Smith, K.A. (1988). Interleukin-2: inception, impact, and implications. Science *240*, 1169–1176.

Sprinzak, D., Lakhanpal, A., Lebon, L., Santat, L.A., Fontes, M.E., Anderson, G.A., Garcia-Ojalvo, J., and Elowitz, M.B. (2010). Cis-interactions between Notch and Delta generate mutually exclusive signalling states. Nature *465*, 86–90.

Sprinzak, D., Lakhanpal, A., LeBon, L., Garcia-Ojalvo, J., and Elowitz, M.B. (2011). Mutual inactivation of Notch receptors and ligands facilitates developmental patterning. PLoS Comput. Biol. *7*, e1002069.

Tkach, K.E., Barik, D., Voisinne, G., Malandro, N., Hathorn, M.M., Cotari, J.W., Vogel, R., Merghoub, T., Wolchok, J., Krichevsky, O., and Altan-Bonnet, G. (2014). T cells translate individual, quantal activation into collective, analog cytokine responses via time-integrated feedbacks. Elife (Cambridge) *3*, e01944.

Villarino, A.V., Stumhofer, J.S., Saris, C.J.M., Kastelein, R.A., de Sauvage, F.J., and Hunter, C.A. (2006). IL-27 limits IL-2 production during Th1 differentiation. J. Immunol. *176*, 237–247.

Wang, R., Rogers, A.M., Rush, B.J., and Russell, J.H. (1996). Induction of sensitivity to activation-induced death in primary CD4+ cells: a role for interleukin-2 in the negative regulation of responses by mature CD4+ T cells. Eur. J. Immunol. *26*, 2263–2270.

Waysbort, N., Russ, D., Chain, B.M., and Friedman, N. (2013). Coupled IL-2-dependent extracellular feedbacks govern two distinct consecutive phases of CD4 T cell activation. J. Immunol. *191*, 5822–5830.

Whitmire, J.K., Benning, N., and Whitton, J.L. (2006). Precursor frequency, nonlinear proliferation, and functional maturation of virus-specific CD4+ T cells. J. Immunol. *176*, 3028–3036.

Whitmire, J.K., Benning, N., Eam, B., and Whitton, J.L. (2008). Increasing the CD4+ T cell precursor frequency leads to competition for IFN-gamma thereby degrading memory cell quantity and quality. J. Immunol. *180*, 6777–6785.

Williams, M.A., Ravkov, E.V., and Bevan, M.J. (2008). Rapid culling of the CD4+ T cell repertoire in the transition from effector to memory. Immunity *28*, 533–545.

Youk, H., and Lim, W.A. (2014). Secreting and sensing the same molecule allows cells to achieve versatile social behaviors. Science *343*, 1242782.

Yui, M.A., Sharp, L.L., Havran, W.L., and Rothenberg, E.V. (2004). Preferential activation of an IL-2 regulatory sequence transgene in TCR gamma delta and NKT cells: subset-specific differences in IL-2 regulation. J. Immunol. *172*, 4691–4699.

Zaretsky, I., Polonsky, M., Shifrut, E., Reich-Zeliger, S., Antebi, Y., Aidelberg, G., Waysbort, N., and Friedman, N. (2012). Monitoring the dynamics of primary T cell activation and differentiation using long term live cell imaging in microwell arrays. Lab Chip *12*, 5007–5015.

Zhu, J., and Paul, W.E. (2008). CD4 T cells: fates, functions, and faults. Blood *112*, 1557–1569.